PHILOSOPHICAL TRANSACTIONS OF THE ROYAL SOCIETY A MATHEMATICAL, PHYSICAL & ENGINEERING SCIENCES

Dimensional Changes in Polycrystalline Graphites under Fast-Neutron Irradiation

B. T. Kelly, W. H. Martin and P. T. Nettley

Phil. Trans. R. Soc. Lond. A 1966 **260**, 51-71
doi: 10.1098/rsta.1966.0029

DIMENSIONAL CHANGES IN POLYCRYSTALLINE GRAPHITES UNDER FAST-NEUTRON IRRADIATION

By B. T. KELLY, W. H. MARTIN and P. T. NETTLEY

United Kingdom Atomic Energy Authority, Reactor Materials Laboratory, Culcheth, Warrington, Lancs.

(*Communicated by H. Kronberger, F.R.S.—Received 4 October 1965—Read 3 March 1966*)

CONTENTS

The changes in dimensions and linear thermal expansion coefficients of several polycrystalline graphites irradiated at 170 and 200 °C are presented. The results are compared with the changes in these parameters which were observed in very highly oriented pyrolytic polycrystalline graphite and were discussed in the preceding paper. The relation between dimensional changes occurring in polycrystalline aggregates and those in a monocrystal is discussed in terms of structural parameters A_x. The variation of these parameters with crystal strain is derived for the different graphites which have been investigated. The analysis shows that, at low crystal strains, *c* axis crystal growth is absorbed by porosity so that the bulk volume changes in the polycrystalline materials are less than those in a single crystal. However, as crystal strain closes the porosity, the rate of bulk volume change approaches that of the single crystal and eventually equals it. At still higher crystal strains nett porosity generation can occur so that the bulk expands at a faster rate than the single crystal. The results also show that the relationship between linear growth rate and the linear thermal expansion coefficient, which has been well established at low crystal strains, breaks down at high strains. However, the results have been used to develop a new model. This enables the crystal dimensional changes to be determined as a function of fast-neutron dose at any irradiation temperature, using bulk dimensional change data from experiments on pile grade A graphite. The crystal strains determined from the new model can be used to predict the dimensional changes of other graphites at other irradiation temperatures from their behaviour at 200 °C.

1. Introduction

The preceding paper (Kelly, Martin & Nettley 1966) discussed the dimensional change behaviour of very highly oriented pyrolytic polycrystalline graphite under fast-neutron irradiation. The knowledge of the behaviour of monocrystalline graphite derived from this work is a necessary prerequisite to the understanding of the dimensional changes occurring in more randomly oriented polycrystalline graphites.

In previous work, after relatively short irradiations (Woods, Bupp & Fletcher 1955; Simmons 1957; Simmons & Reynolds 1962), the rates of change of dimensions of polycrystalline graphites at a particular irradiation temperature have been shown to correlate with the linear thermal expansion coefficients of these graphites. According to Simmons

(1957, 1961), the strain in the direction x in a polycrystalline aggregate, during dose $d\gamma$, due to strains in the crystals is given by

$$g_x = A_x g_c + (1 - A_x)\, g_a, \tag{1}$$

where $g_x = (1/l_x)\,(dl_x/d\gamma)$ is the fractional increase in length l_x in the direction x in the aggregate per unit dose,

$g_c = (1/X_c)\,(dX_c/d\gamma)$ is the fractional increase in length in the c axis direction of a crystal per unit dose,

$g_a = (1/X_a)\,(dX_a/d\gamma)$ is the fractional increase in length in the a axis direction of a crystal per unit dose,

A_x is a parameter which depends on the type of graphite, the direction of cut relative to the moulding or extrusion direction, and on the irradiation dose and temperature; it is a measure of the distribution of an applied load in the direction x between the c and a axis crystal directions in the aggregate. Similarly, the linear thermal expansion coefficient, α_x, of the graphite aggregate in the direction x, in the same irradiated state, is related to the crystal thermal expansion coefficients α_c and α_a, in the c and a axis directions respectively, by

$$\alpha_x = A_x \alpha_c + (1 - A_x)\, \alpha_a; \tag{2}$$

A_x is the same parameter as that given in equation (1).

The available experimental evidence with reference to Simmons's theory was discussed by Simmons, Kelly, Nettley & Reynolds (1964). They used the observed irradiation-induced changes in bulk dimensions and linear thermal expansion coefficients in the directions perpendicular and parallel to extrusion in British Reactor Grade graphite, *PGA* (cf. O'Driscoll & Bell 1960), in (1) and (2) to determine the crystal strains as a function of dose. They found that the shapes of the curves of strain in *PGA* crystals, as a function of dose, were similar to those observed for pyrolytic graphite but that, at all doses at 200 °C, the *PGA* crystals exhibited larger strains than the pyrolytic material.

We have now measured the changes in bulk dimensions and linear thermal expansion coefficients in several polycrystalline graphites as a function of neutron dose at irradiation temperatures of 170 and 200 °C. Graphites having a wide range of thermal expansion coefficients have been studied. In addition, we have measured the helium density of *PGA* material as a function of neutron dose. The latter experiment shows clearly that the crystal strains derived from (1) and (2) are too large after crystal strains of 0·15 have been exceeded. Consequently, we have examined why the equations break down at large crystal strains. We have developed a model which enables us to retain (1) and to determine A_x as a function of total strain in the crystals of the different graphites which have been investigated. It will be shown that this model yields a reasonable physical explanation of the results; it can be used to determine the high temperature irradiation behaviour of graphites from their behaviour at 200 °C, if the behaviour of their crystals at the high temperatures is known, or, alternatively, to estimate the crystal strain behaviour at high temperatures from dimensional change data.

2. Experimental

The polycrystalline graphites studied were all manufactured from cokes, binders and impregnants (Currie, Hamister & MacPherson 1955), which yield well-graphitized products; they are listed in table 1. The materials include a moulded, very highly oriented

graphite, *ZTA* (Bushong & Neel 1962); an extruded anisotropic graphite which has a relatively low volume thermal expansion coefficient, *PGA* (O'Driscoll & Bell 1960); a moulded isotropic graphite with a high volume thermal expansion coefficient, *RB* (Hutcheon & Jenkins 1965); a moulded isotropic graphite (*MHLM*), with a low volume thermal expansion coefficient, *HM* (cf. Eatherly *et al.* 1958); and an extruded graphite, *TC* (cf. Legendre *et al.* 1955), which represents conditions of isotropy and thermal expansion intermediate between the conditions represented by the *PGA* and *HM* materials. The boron contents of all the materials were much lower than the level at which there is a significant effect on the rate of accumulation of irradiation defects (cf. Thrower 1964).

TABLE 1. PHYSICAL PROPERTIES OF THE GRAPHITES BEFORE IRRADIATION

		anisotropic graphites			near-isotropic graphites	
reference code	...	*PGA*	*ZTA*	*TC*	*RB*	*HM*
description		pile grade A (Shell H 100 petroleum coke) extruded	*ZTA* recrystallised moulded	Texas coke (doubly impregnated) extruded	uncalcined coal tar pitch coke and coal tar pitch binder moulded	*MHLM* Texas coke moulded
source		U.K.A.E.A.	National Carbon Company	Société Pechiney	Reactor Materials Laboratory, Culcheth	Great Lakes Carbon Company
thermal expansion coefficient (20 to 120 °C) (10^{-6} degC^{-1})	∥	0·8	9·2	2·5	5·6	3·0
	⊥	2·8	0·5	3·8	5·5	2·5
thermal conductivity (cal cm^{-1} s^{-1} degC^{-1})	∥	0·5	0·15	0·40	0·25	0·36
	⊥	0·3	0·5	0·33	0·25	0·38
electrical resistivity (mΩ cm)	∥	0·6	2·3	0·7	1·5	0·8
	⊥	1·0	0·6	0·9	1·5	0·7
Young's modulus (10^5 Lb/in.^{2})	∥	17	7	—	29	—
	⊥	8	30	—	29	—
density (g/cm^3)		1·7	1·9	1·7	1·8	1·8

The irradiation techniques, the apparatus used for determining dimensions and thermal expansion coefficients and the method of determining fast-neutron dose are identical to those described for pyrolytic graphite in the preceding paper. Open pore volume measurements were made on *PGA* graphite specimens using the method described by Ashton & Winton (1961). The techniques used for measuring the physical properties prior to irradiation have been described previously (Kelly, Jones & James 1962). The specimens were 0·25 in. in diameter and between 0·5 and 3·0 in. long with lapped ends.

Physical properties of the materials before irradiation are given in table 1. Directional properties in the materials refer to the directions perpendicular or parallel to the direction of moulding or extrusion.

Changes in the dimensions and linear thermal expansion coefficients of *PGA* graphite during irradiation at temperatures in the range 150 to 650 °C have already been reported (Simmons *et al.* 1964). In the temperature range 300 to 650 °C these data have been extended in dose; the dimensional changes are shown in figure 1. Changes in the dimensions

and thermal expansion coefficients of the other graphites induced by irradiation at temperatures of 170 and 200 °C, are presented as a function of fast-neutron dose in figures 2 to 10. Changes in open pore volume of *PGA* graphite during irradiation at 200 °C are given in table 2.

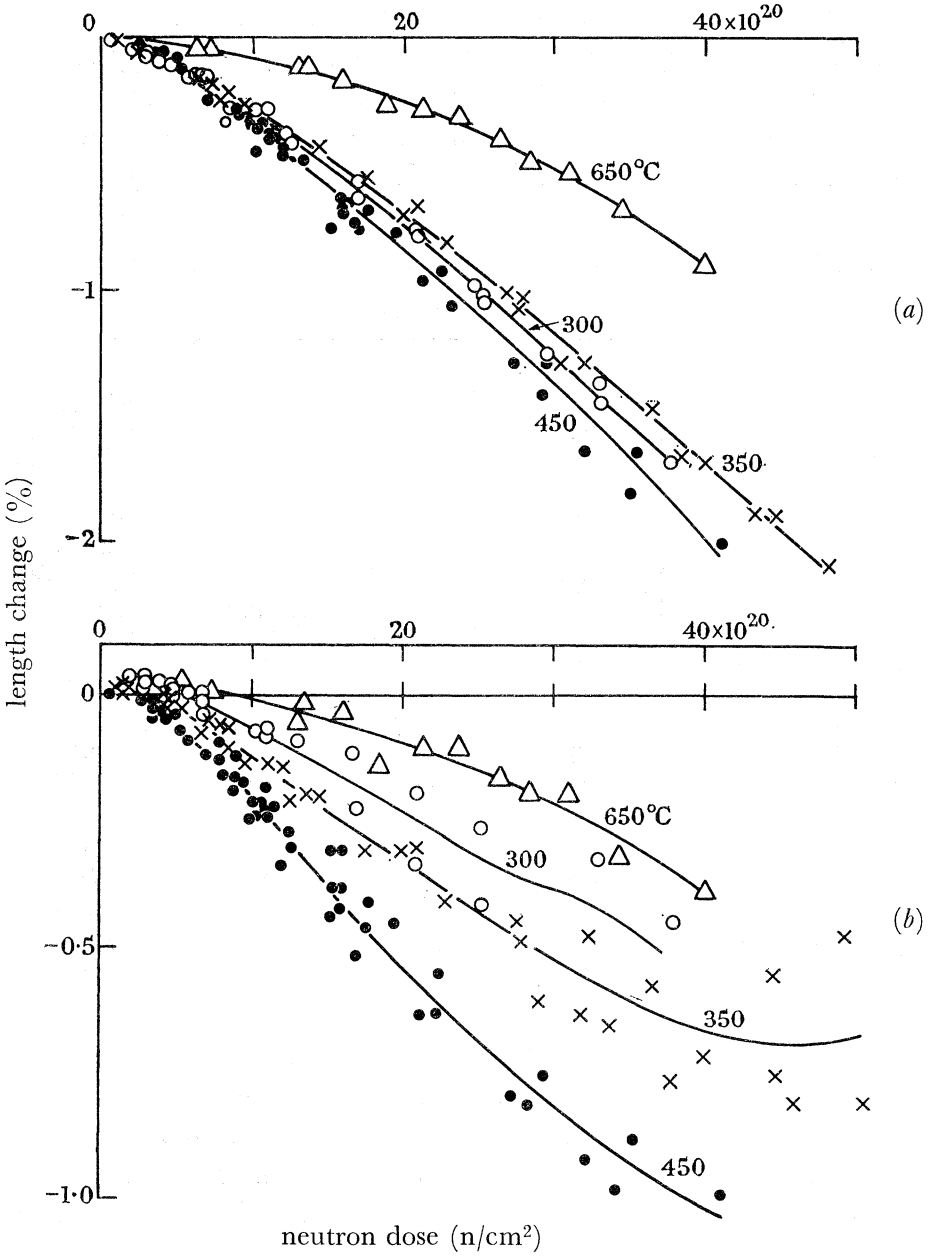

FIGURE 1. Dimensional changes induced in *PGA* graphite by neutron irradiation in the temperature range 300 to 650 °C. (*a*) Parallel to extrusion; (*b*) perpendicular to extrusion.

3. Comparison of results on *PGA* material with theory

Data on the irradiation induced changes in dimensions and thermal expansion coefficients in *PGA* graphite can be used in (1) and (2) to determine the crystal strains $\Delta X_c/X_c$ and $\Delta X_a/X_a$ in the *c* and *a* axis directions as a function of neutron dose. A complete analysis requires a knowledge of the variations of α_c and α_a in *PGA* crystals with irradiation dose. These functions are not known for *PGA* material, but they are known for pyrolytic graphite

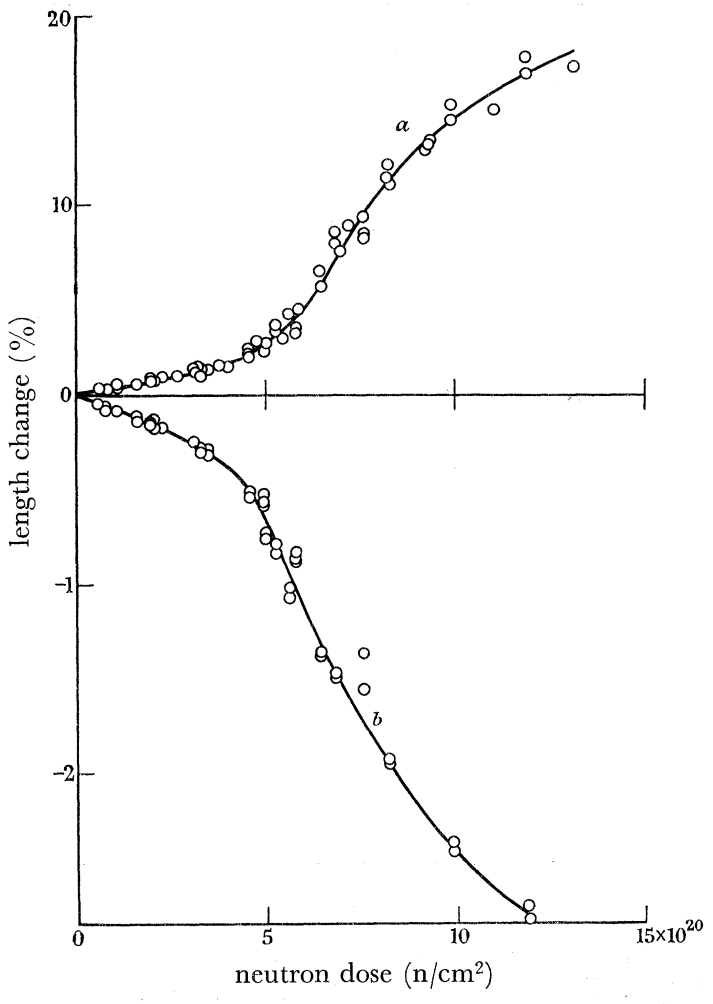

FIGURE 2. Dimensional changes induced in *ZTA* graphite by neutron irradiation at 200 °C. (*a*) Parallel to pressing; (*b*) perpendicular to pressing.

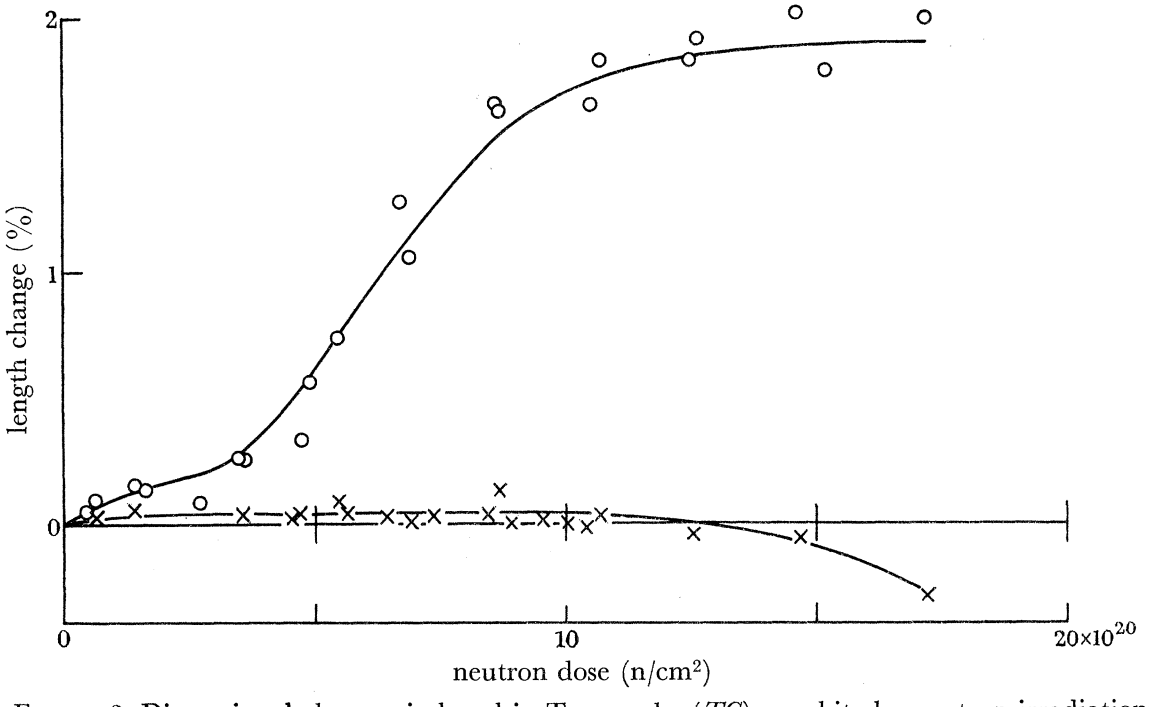

FIGURE 3. Dimensional changes induced in Texas coke (*TC*) graphite by neutron irradiation at 200 °C. ×, Parallel to extrusion; ○, perpendicular to extrusion.

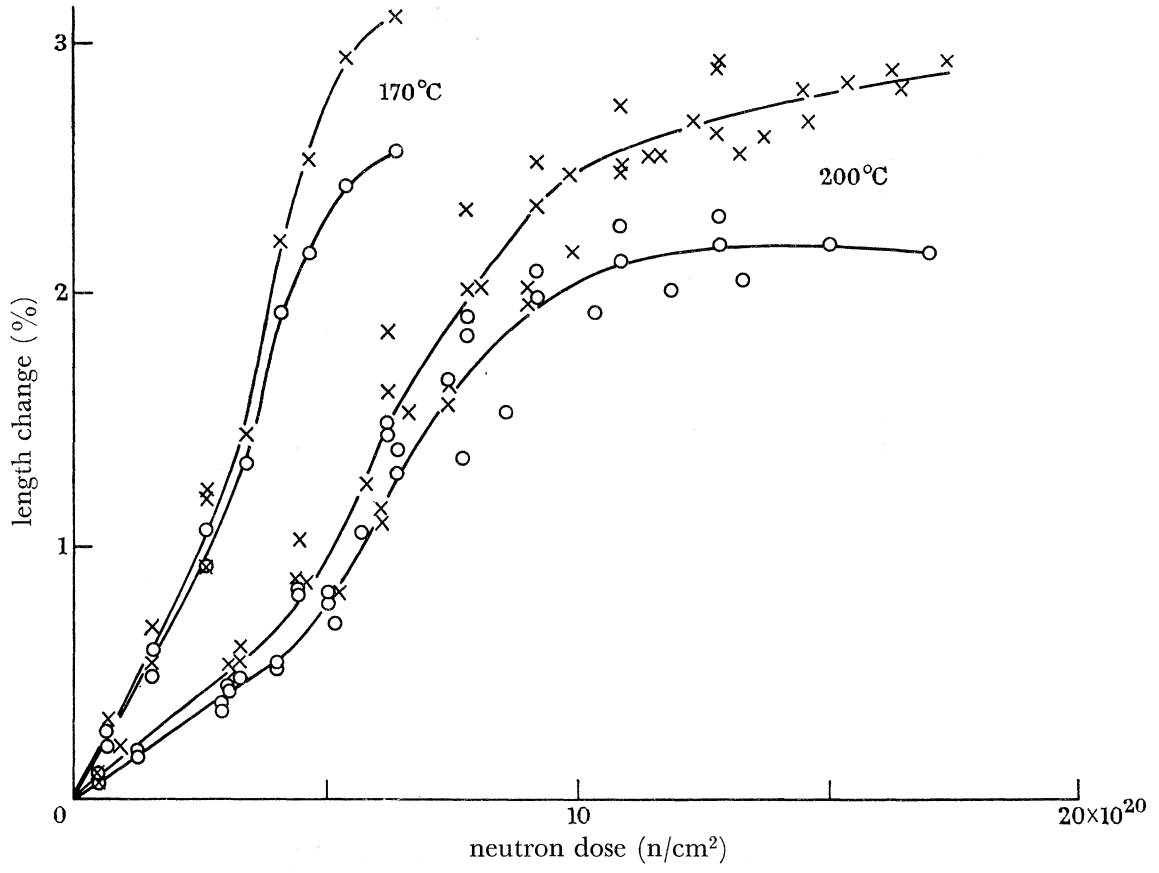

FIGURE 4. Dimensional changes induced in *RB* graphite by neutron irradiation at 170 and 200 °C. ×, Parallel to pressing; ○, perpendicular to pressing.

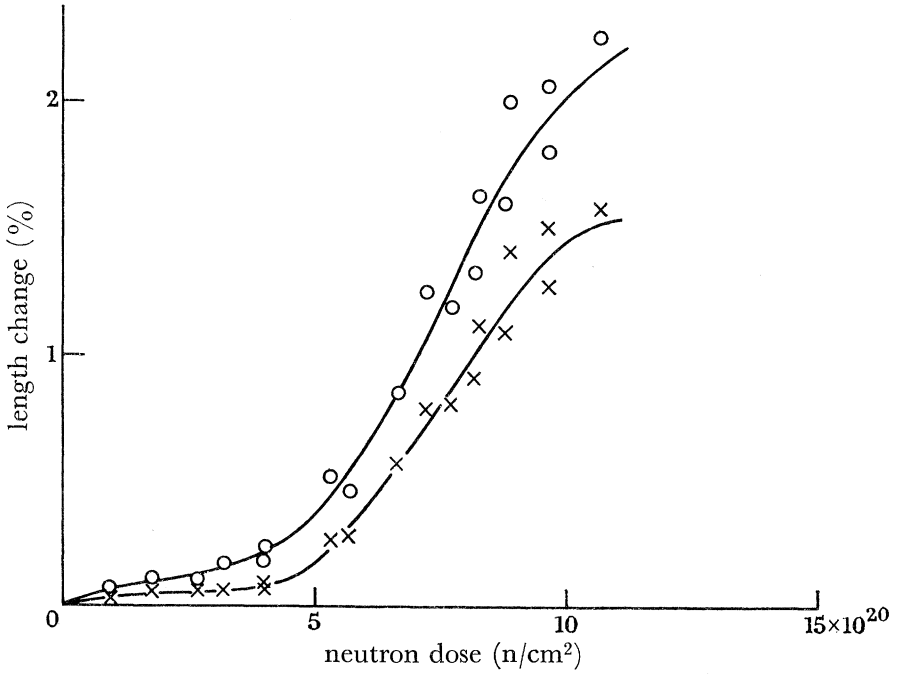

FIGURE 5. Dimensional changes induced in *MHLM* (*HM*) graphite by neutron irradiation at 200 °C. ○, Parallel to pressing; ×, perpendicular to pressing.

at an irradiation temperature of 200 °C. Detailed differences in crystal structure in different graphites may cause $\Delta X_c/X_c$, $\Delta X_a/X_a$, α_c and α_a to be different functions of dose in different materials. Differences in $\Delta X_c/X_c$ and $\Delta X_a/X_a$ between pyrolytic and *PGA* graphite crystals

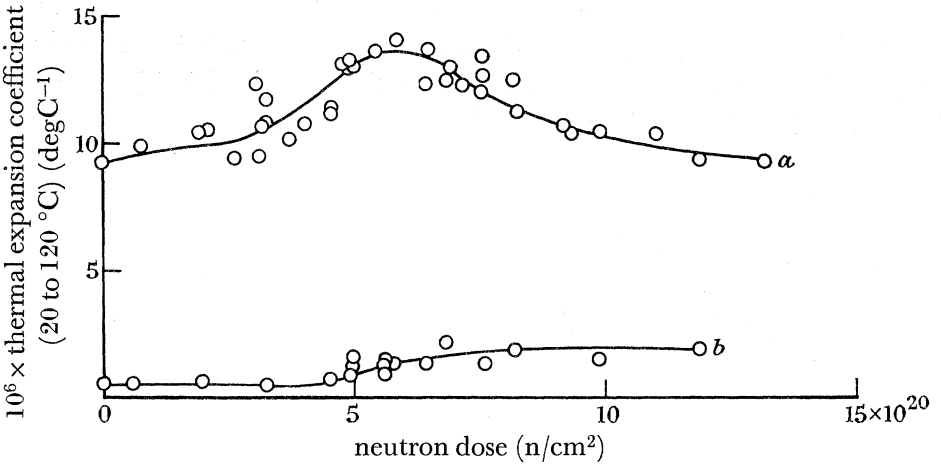

FIGURE 6. Variation of thermal expansion coefficients of *ZTA* graphite with neutron dose at 200 °C. (*a*) Parallel to pressing; (*b*) perpendicular to pressing.

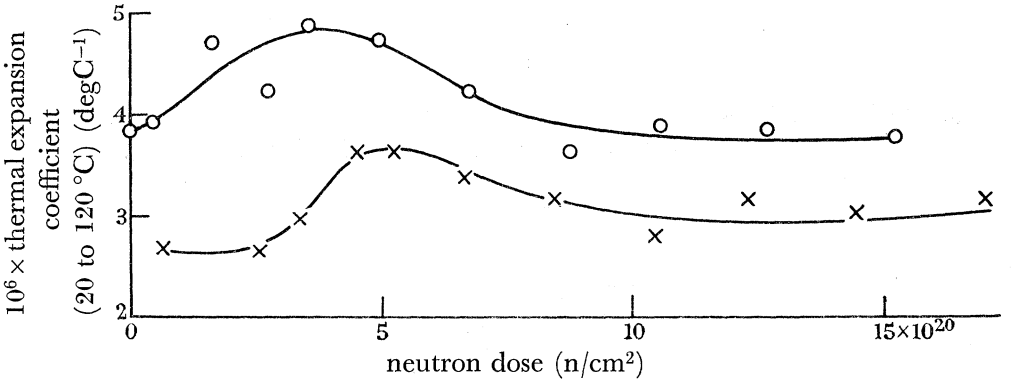

FIGURE 7. Variation of thermal expansion coefficients of Texas coke (*TC*) graphite with neutron dose at 200 °C. ×, Parallel to extrusion; ○, perpendicular to extension.

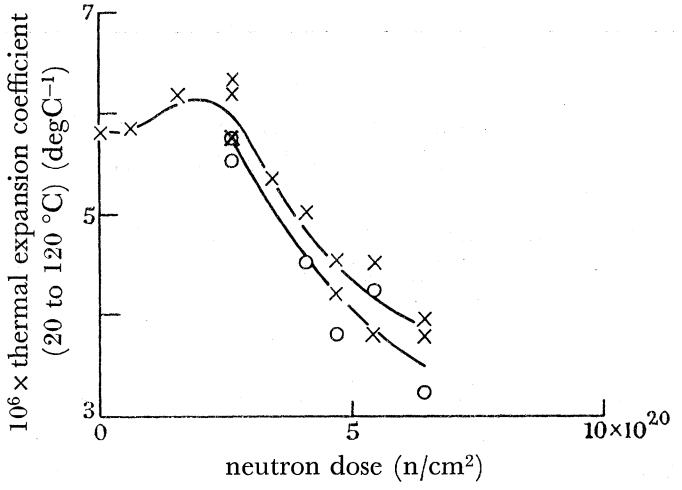

FIGURE 8. Variation of thermal expansion coefficients of *RB* graphite with neutron dose at 170 °C. ×, Parallel to pressing; ○, perpendicular to pressing.

have been observed previously (Simmons *et al.* 1964). In the present analysis we have, therefore, assumed that α_c is a unique function of $\Delta X_c/X_c$ and α_a is a unique function of $\Delta X_a/X_a$ in all well-graphitized materials; these functions are obtained from the data on pyrolytic graphite given in the preceding paper. It is considered that these assumptions give the best possible method of using pyrolytic graphite thermal expansion data to determine the variation of A_x in polycrystalline aggregates with dose; they are justified by the mechanisms postulated to explain the changes in α_c and α_a in the preceding paper.

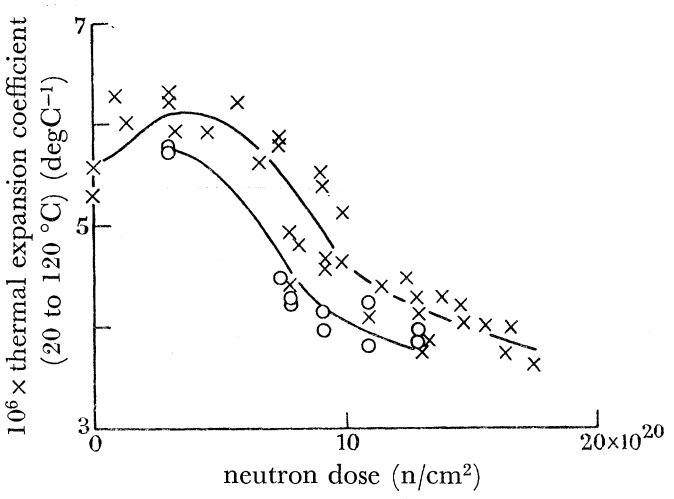

FIGURE 9. Variation of thermal expansion coefficients of *RB* graphite with neutron dose at 200 °C. ×, Parallel to pressing; ○, perpendicular to pressing.

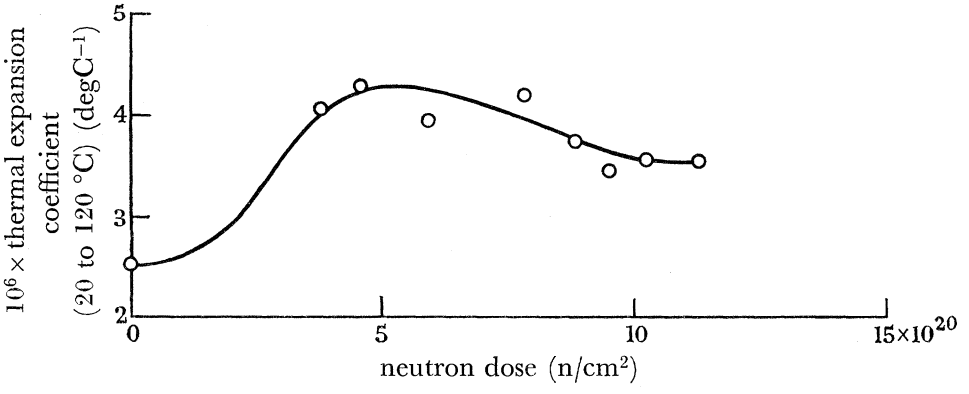

FIGURE 10. Variation of thermal expansion coefficient of *MHLM* (*HM*) graphite perpendicular to pressing with neutron dose at 200 °C.

The variations of α_c and α_a with their corresponding crystal strains have been used with the experimental data on *PGA* material at 200 °C in (1) and (2). The equations have been solved by using successive approximations and integrations to yield $\Delta X_c/X_c$, $\Delta X_a/X_a$, $A_\perp$ and $A_\parallel$ as functions of dose at 200 °C; $A_\perp$ and $A_\parallel$ are the values of A_x in the directions perpendicular and parallel to the extrusion direction respectively.

In figure 11 we have compared the *c* and *a* axis crystal strains derived in this way for *PGA* graphite with the dimensional changes observed in pyrolytic material. The data from the two materials have the same form but the calculated *PGA* crystal strains are clearly much larger than those in pyrolytic material particularly at high dose.

The validity of the calculated *PGA* crystal strains can easily be tested. We note that, at high doses, the calculated *PGA* crystal density approaches the density of the *PGA* graphite aggregate. The helium density results given in table 2 show clearly that this is not correct. In order to explain this discrepancy we must now examine the pore structure of *PGA* material in more detail.

TABLE 2. CHANGES IN OPEN PORE VOLUME OF *PGA* GRAPHITE DURING IRRADIATION AT 200 °C

specimen	fast-neutron dose (10^{20} n/cm^2)	open pore volume† (cm^3/100 cm^3)	helium density‡ (g/cm^3)
1	1·8	20·4	2·11
	3·0	20·8	2·12
2	4·1	15·8	2·07
	5·3	15·4	2·06
3	9·6	13·8	1·99
	11·0	11·7	1·94
	12·2	13·0	1·96
	12·2	powdered sample	1·95
4	10·8	13·5	1·97
	12·0	15·0	2·01
5	13·6	16·3	1·99
	15·1	14·7	1·94
	16·2	16·4	1·96
	16·2	powdered sample	1·97
6	19·9	14·1	1·94
	21·8	15·3	1·97
	23·0	14·9	1·95
	23·0	powdered sample	1·95

The samples investigated were 2·5 to 3 in. long and 0·25 in. in diameter.

† The error in open pore volume measurement is about ±10 %.

‡ The error in helium density measurement is ±1 %.

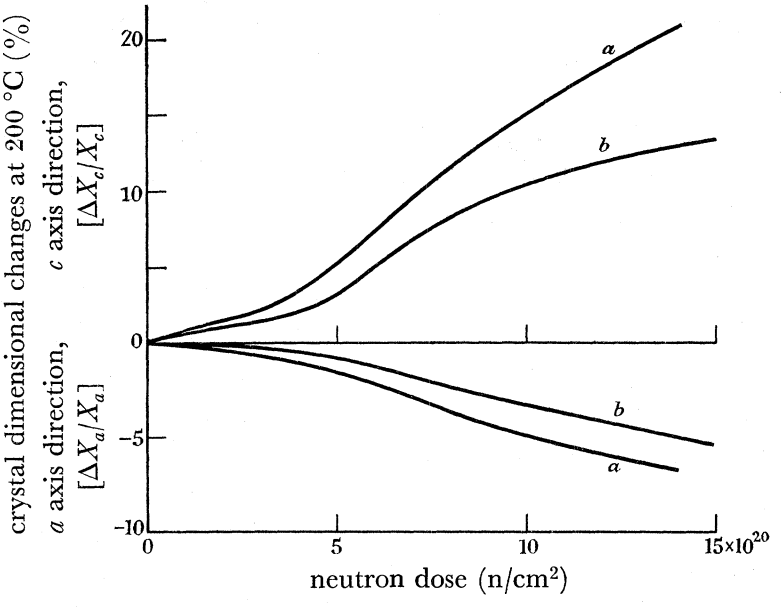

FIGURE 11. Crystal dimensional changes calculated from thermal expansion and dimensional change data for *PGA* graphite (curves *a*), compared with the dimensional changes observed in pyrolytic graphite at 200 °C (curves *b*).

When the specific volume of a graphite specimen is measured in helium, some of the porosity, amounting to about 20% of the bulk volume in *PGA* graphite, is penetrated by the helium. Therefore, the volume which is determined is that of the crystals together with any closed porosity which the crystals contain. If the graphite is finely powdered before measurement, some of this closed porosity is opened so that the measured density is then even closer to the true density.

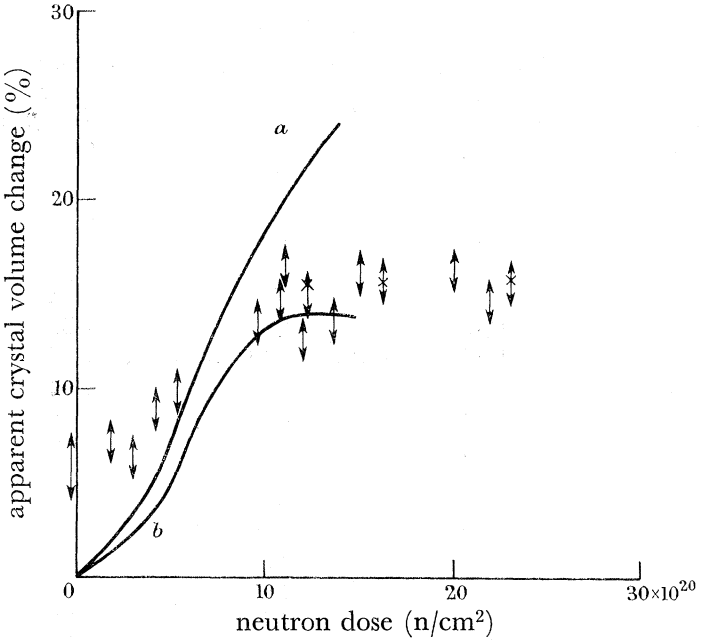

FIGURE 12. Variation of apparent crystal volume with neutron dose. Comparison of helium density measurements with volume changes observed in pyrolytic graphite (curve *b*) and those calculated from *PGA* graphite data, thermal expansion being used to determine A_x (curve *a*). ↕, Apparent crystal volume change (including some closed porosity) from helium density measurements. Error limits are from helium density measurement errors; ×, from helium density measurement on this specimen after grinding to a particle size less than 0·0029 in. (200 mesh).

The unirradiated *PGA* crystal density, determined from lattice parameter measurement using X-rays is 2·26 g/cm³ and the helium density is 2·15 g/cm³, so that the closed porosity is about 5%. Crystal strain during irradiation fills this closed porosity (Sutton & Howard 1962) so that the helium density measurements underestimate the true crystal densities by an amount which decreases with irradiation dose. In figure 12 upper limits for the crystal volume changes in *PGA* graphite, calculated on the assumption that before irradiation the crystal density was 2·26 g/cm³, have been plotted as a function of fast-neutron dose using the data given in table 2. They are compared with the volume changes observed in pyrolytic graphite and those calculated from the *PGA* crystal data shown in figure 11. The values of crystal volume change in *PGA* material obtained from helium density measurements tend to be too high because closed porosity has been neglected. This is particularly so at low doses where crystal strains have not closed up the initial inaccessible porosity. Therefore, it is clear from figure 12 that the crystal volume changes obtained using (1) and (2) and the irradiation data are too large at high doses. This is the observation which we must now try to explain.

4. Discussion

The fact that a combination of (1) and (2) yields crystal strains which are too large at high doses does not necessarily mean that the equations are completely incorrect. It is much more likely that, at high crystal strains, the values of A_x which must be used in (1) are larger than those obtained from thermal expansion measurements and (2), even after allowing for the irradiation induced changes in crystal thermal expansion coefficients. We have assumed that this is why we obtain crystal strains which are too large at high dose.

The reason for thermal expansion and (2) giving apparent low A_x values, when applied to dimensional changes at high crystal strains, is difficult to ascertain. Let us first consider the parameters other than A_x in (2). It may be that the changes in crystal thermal expansion coefficients in *PGA* graphite are significantly larger than those observed in pyrolytic graphite, but this does not seem to be a reasonable hypothesis. At a crystal c axis strain of about 0·25, the value of α_c would have to be $10 \times 10^{-6}\,\mathrm{degC}^{-1}$, to give reasonable crystal dimensional changes in *PGA* graphite, whereas the lowest value observed in pyrolytic graphite at the same order of crystal strain at 170 or 200 °C is about $16 \times 10^{-6}\,\mathrm{degC}^{-1}$.

An alternative explanation may result from the fact that the thermal expansion coefficients were measured at temperatures (20 to 120 °C) significantly below the irradiation temperature. This may have caused an error in the determination of A_x because porosity which was closed by irradiation-induced crystal strain could be partially opened on cooling from the irradiation temperature. Investigation of this effect has shown, however, that the increase in apparent A_x obtained by measuring the thermal expansion coefficient at the irradiation temperature, but out-of-pile, is only small.

A more reasonable explanation is that thermal expansion measurements and (2) give the correct value of A_x as they do at lower crystal strains, but that an additional mechanism of dimensional change is present. In bromination studies (Brocklehurst & Bishop 1964), A_x values have been observed at high crystal strains which are significantly larger than those derived from thermal expansion measurements on irradiated material. The larger A_x values observed in the bromination tests may be unequivocally attributed to the generation of porosity produced because of the incompatibility of the crystal growth with that of the aggregate. The length changes due to the volume of the new porosity will appear in (1) as an apparent increase in A_x.

If the thermal expansion coefficient were measured in the pile, in the presence of the fast-neutron flux and at the irradiation temperature, the state of internal stress in the graphite would be identical to that present during the production of the dimensional changes. In this case, the same effective A_x should apply to thermal expansion and dimensional change measurements. If the irradiation creep which occurs in graphite (Reynolds 1965) plays a significant role in porosity generation or in the restraint of thermal expansion of the crystals, the rate of change of temperature in the in-pile measurement of thermal expansion would have to be such that thermally induced rates of change of crystal dimensions approximate to the irradiation-induced rates of change of crystal dimensions.

In order to proceed further, it is necessary to derive the A_x values appropriate to irradiation growth, from dimensional change measurements using (1), rather than from thermal expansion data and (2). This requires a knowledge of the variation with neutron dose at

PHILOSOPHICAL TRANSACTIONS OF THE ROYAL SOCIETY A MATHEMATICAL, PHYSICAL & ENGINEERING SCIENCES

200 °C, of the crystal dimensional changes in *PGA* graphite. The simplest assumption which may be made is that the crystal dimensional changes in *PGA* are the same as those observed in pyrolytic graphite. However, up to doses of about 3×10^{20} n/cm^2 at 200 °C, α_c and α_a do not change significantly and little change is observed in the bulk linear thermal expansion coefficients of *PGA* graphite. This implies that A_x is unchanged over this dose range and that, at these small crystal strains, thermal expansion data can be used in (2) to determine A_x; the crystal dimensional changes can then be obtained from (1). In this dose range,

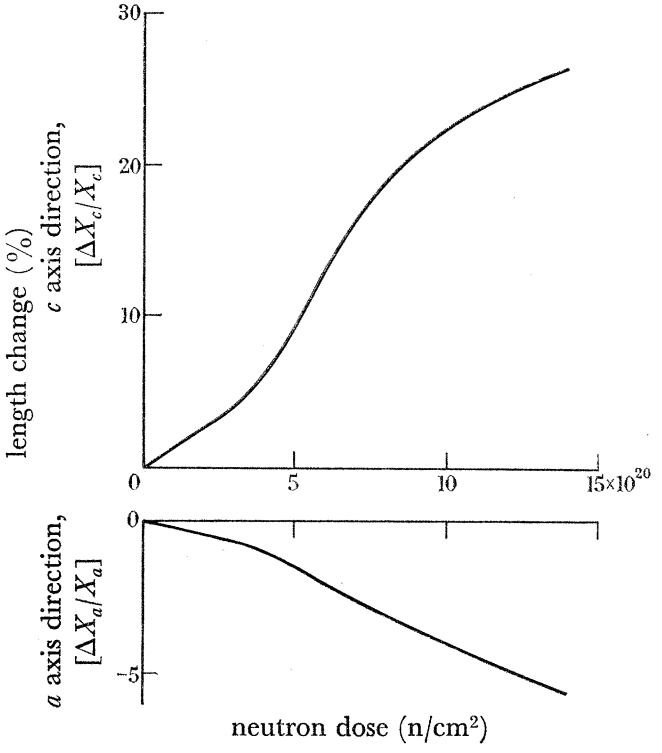

FIGURE 13. Crystal dimensional changes at 200 °C calculated from *PGA* graphite data at low doses and using pyrolytic graphite dimensional change rates after a *c* axis strain of 4%.

where helium density measurements give us no help, the calculated rates of crystal strain with dose in *PGA* graphite are significantly larger than those observed in pyrolytic graphite, and since the crystal strains are low, it is considered that these differences in crystal strain rates in the two materials are real. This belief is further substantiated by the fact that, if the pyrolytic graphite dimensional changes are used in (1) with the *PGA* bulk data, the A_x values decrease with dose at low doses. Since A_x should continually increase as a result of porosity closure, this picture is physically unacceptable.

However, figure 12 shows that, at least at high doses, when most of the microporosity has been closed by crystal strain, the crystal volume changes measured by helium density in *PGA* graphite are very similar to those observed in pyrolytic graphite. Helium density measurements on bulk and finely powdered samples of *PGA* graphite irradiated to high dose at 200 °C yield the same results, thus showing that there is negligible closed porosity when the crystal strains are large. It is seen from figure 11 that, at *c* axis crystal growths in excess of 4%, the rate of crystal strain with dose increases markedly. It seems possible, therefore, that to a first approximation, the rate of accumulation of further *c* axis strain,

in excess of 4%, is governed mainly by the irradiation damage that is present, rather than by the initial properties of the crystals. Therefore, in order to form the basis for relating dimensional changes in the polycrystalline *PGA* aggregate with those in the crystals, it is postulated that the rates of change of crystal strain in *PGA* and pyrolytic graphites are different up to a *c* axis crystal strain of 4%, but that above this strain the damage mechanism is modified and crystals in the two materials behave identically. This hypothesis is supported by other work (Goggin, Henson, Perks & Reynolds 1964). Their data indicate that graphites which exhibit high crystal strain rates at low doses at 200 °C, show less tendency for acceleration in rates of crystal strain with dose at 4% *c* axis strain than do graphites which exhibit lower initial crystal strain rates.

In the present analysis, the crystal dimensional changes in *PGA* graphite at 200 °C up to 4% *c* axis strain have been obtained using thermal expansion measurements to derive the A_x coefficients. At higher *c* axis strains, the rates of crystal dimensional change with dose observed in pyrolytic graphite have been used. However, the ratio $\delta = -g_a/g_c$ at low dose is different in *PGA* and pyrolytic graphites; therefore the level of $\Delta X_c/X_c$ at which acceleration in crystal strain rates takes place has been chosen to define the dose at which the rates of crystal strain with dose in *PGA* graphite become equal to those in pyrolytic graphite. This means that the level of $\Delta X_a/X_a$ at this dose is different in the two graphites. The crystal dimensional changes in *PGA* material obtained by this method are shown in figure 13.

5. The behaviour of other graphites

Analysis of the data on the other anisotropic materials which were irradiated shows that their initial rates of crystal strain with dose are either similar to those of *PGA* graphite or they lie between the values for *PGA* and pyrolytic materials. The analysis cannot be applied to isotropic materials. The irradiation data in figures 2 to 5 can be used to compare the volume changes in the polycrystalline graphites with those in pyrolytic material as a function of irradiation dose at 200 °C. Figure 14 shows the bulk volume increase in all the materials as a function of total crystal strain X_T. X_T equals $\Delta X_c/X_c - \Delta X_a/X_a$; it is a measure of the crystal shape change upon which A_x is assumed to depend (cf. Martin, Kelly & Nettley 1962). Figure 15 shows the difference between the volume changes observed in pyrolytic material and those observed in the artificial graphites, also as a function of X_T. For simplicity, it has been assumed that the crystal changes given in figure 13 apply to all well-graphitized polycrystalline materials and these have been used to derive the X_T values for these materials. Figures 14 and 15 show that, at low crystal strains, microporosity absorbs part of the *c* axis strain in the artificial graphites, so that the volume changes in the polycrystalline materials are less than those in single crystals. As X_T increases, the microporosity is filled and the difference between rates of change of bulk volume and crystal volume decreases with crystal strain and eventually becomes zero. With the exception of *ZTA*, values of X_T in excess of 0·27 are required before accommodation of *c* axis strains is complete. In *ZTA*, which is a hot-worked recrystallized material, accommodation of *c* axis strain is complete when $X_T = 0{\cdot}15$. The results also show that, when all the microporosity has been filled and accommodation of *c* axis strain is complete, further crystal strain tends to give rise to bulk changes in the artificial graphites which

are larger than those observed in pyrolytic graphite. This is seen in figure 15 at high crystal strains when the difference between the crystal and bulk changes decreases. Thus, in this condition, further crystal strain in the artificial materials can only be accommodated by

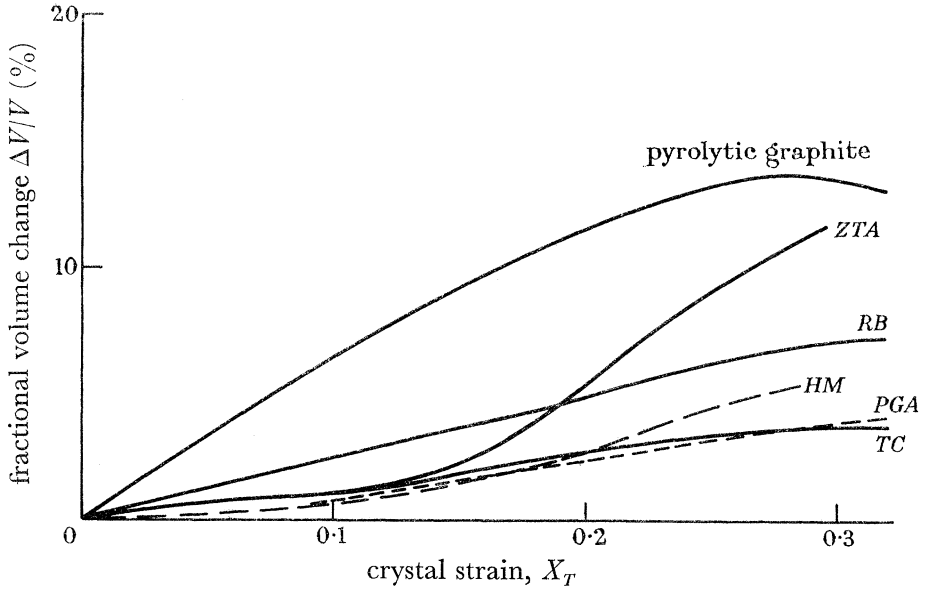

FIGURE 14. Volume changes in graphites as a function of differential crystal strain X_T during irradiation at 200 °C.

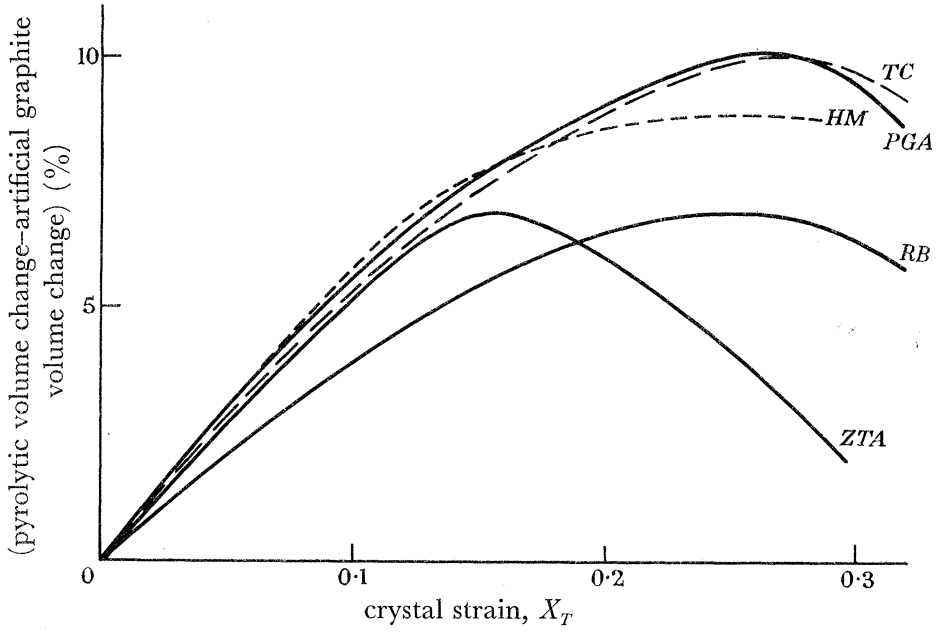

FIGURE 15. Difference in volume changes between pyrolytic and other graphites as a function of differential crystal strain X_T during irradiation at 200 °C.

porosity generation. The helium density measurements on high dose solid and powdered material show that this generated porosity is accessible to helium in *PGA* graphite.

An alternative presentation of the data can be made in the following way: It has again been assumed that the crystal dimensional changes given in figure 13 apply to all the artificial graphites investigated and that they can be used with the bulk dimensional

change data at 200 °C in (1) to derive the A_x parameters as a function of X_T. This has been done for all the graphites investigated and the results are shown in figure 16 (*a* to *d*) together with the values obtained from thermal expansion data in (1) and (2) combined. Since

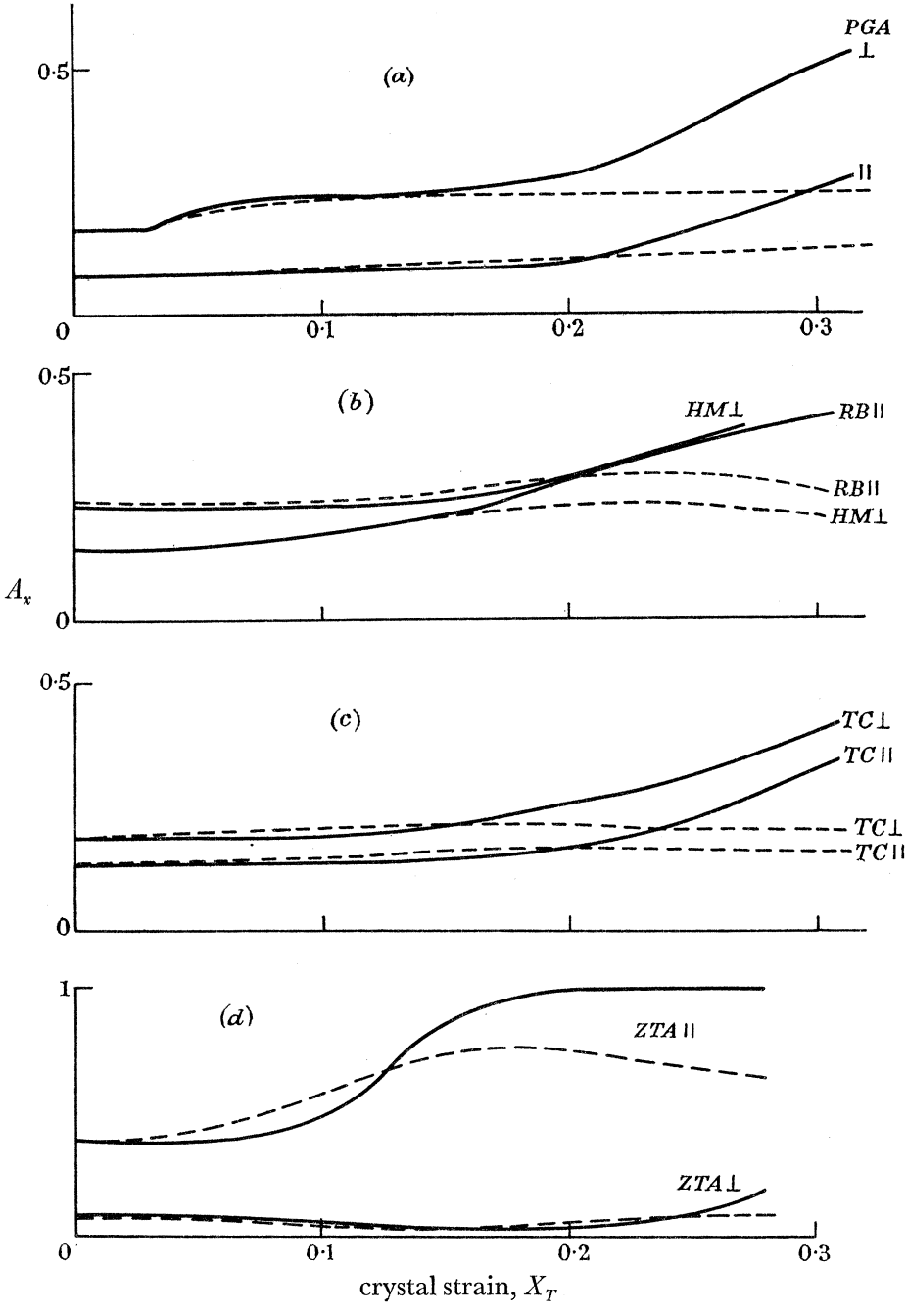

FIGURE 16. Variation of structural parameter A_x with crystal strain X_T for some widely different polycrystalline graphites. (*a*) *PGA* graphite; (*b*) *RB* and *HM* graphites; (*c*) *TC* graphite; (*d*) *ZTA* graphite. The dashed lines are from thermal expansion data.

materials *HM* and *RB* are substantially isotropic, only one direction in these materials has been analysed. At low crystal strains the two methods do of course agree for *PGA* graphite because the treatment makes them do so.

The results show that at low crystal strains ($< 0{\cdot}15$), and for all the materials, the A_x parameters determined by the two methods are very similar. Thus the data are consistent with the hypothesis that (1) and (2) are substantially correct at low crystal strains and that the crystal changes given in figure 13 apply to all the materials except pyrolytic graphite. At high strains, however, the values of A_x obtained from the crystal dimensional changes given in figure 13 are significantly higher than those given by (2) and the thermal expansion data. The higher values present a physically acceptable picture in terms of initial porosity closure and subsequent porosity generation and the variation of A_x with X_T is similar, but not identical, to those obtained on the same materials in bromination studies (Brocklehurst & Bishop 1964). It is interesting to note that $A_x = 1$ in the highly oriented *ZTA* material in the direction parallel to pressing when $X_T > 0{\cdot}20$, thus showing that this material exhibits single crystal *c* axis growth in this direction at high crystal strains.

6. Application of the results to other temperatures

It can easily be seen from equation (1) that the difference in dimensional change rates $g_\perp$ and $g_\parallel$, in the directions perpendicular and parallel respectively to moulding or extrusion, is given by the following equation:

$$\begin{aligned} g_\perp - g_\parallel &= (A_\perp - A_\parallel)(g_c - g_a) \\ &= (A_\perp - A_\parallel)\, g_T. \end{aligned}$$

Now $A_\perp$ and $A_\parallel$ should be unique functions of X_T (cf. Martin *et al.* 1962), and therefore, to a first approximation (for $\Delta l/l \ll 1$, $\ln(1+\Delta l/l) \simeq \Delta l/l$), on integration,

$$G_\perp - G_\parallel = \left(\frac{\Delta l}{l}\right)_\perp - \left(\frac{\Delta l}{l}\right)_\parallel = f(X_T). \tag{3}$$

Therefore, if *PGA* graphite is irradiated under any conditions, the crystal strain X_T can be obtained from the bulk dimensional changes using figure 17, in which $f(X_T)$ is plotted against X_T; this figure has been constructed from figure 13 and the previously published bulk dimensional change data on *PGA* graphite at 200 °C. In addition, the bulk volume change rate in *PGA* graphite is

$$\frac{1}{V}\frac{\mathrm{d}V}{\mathrm{d}\gamma} \simeq 2g_\perp + g_\parallel = (2A_\perp + A_\parallel)\, g_T + 3g_a.$$

On integration this yields, again to a first approximation,

$$\frac{\Delta V}{V} - 3\frac{\Delta X_a}{X_a} = F(X_T). \tag{4}$$

In figure 18, $F(X_T)$ for *PGA* graphite is plotted against X_T using the data given in figure 13 and the bulk dimensional changes in *PGA* graphite at 200 °C. The data on *PGA* graphite have been used because this is the material which has been most extensively irradiated in the U.K.A.E.A. programme on graphite. Figures 17 and 18 can now be used to determine $\Delta X_c/X_c$ and $\Delta X_a/X_a$ from any set of dimensional change data yielding both $G_\perp$ and $G_\parallel$ on *PGA* graphite. Equation (3) gives X_T and then (4) yields $\Delta X_a/X_a$ and hence $\Delta X_c/X_c$.

The latest dimensional change data on *PGA* graphite in the temperature range 300 to 650 °C are presented in figure 1. Data at lower temperatures have been given previously

(Simmons *et al.* 1964). These data have been used to determine $\Delta X_c/X_c$ and $\Delta X_a/X_a$ as functions of dose at different irradiation temperatures and the results, shown as full lines, are compared with the changes observed in pyrolytic graphite, shown as points, under the same conditions of irradiation in figure 19. This figure also includes data on pyrolytic material irradiated in the temperature range 400 to 450 °C in BR-2 (Gray, Hanstock, Kelly & Nettley 1966). The agreement is seen to be reasonably good particularly in the *a* axis direction above 250 °C. At temperatures of 250 °C and below, the initial rates of crystal strain with dose in both directions in *PGA* material appear to be significantly larger

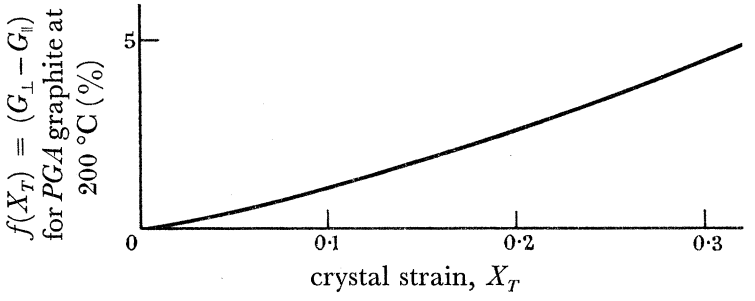

FIGURE 17. Variation of $f(X_T)$ with differential crystal strain X_T for *PGA* graphite irradiated at 200 °C.

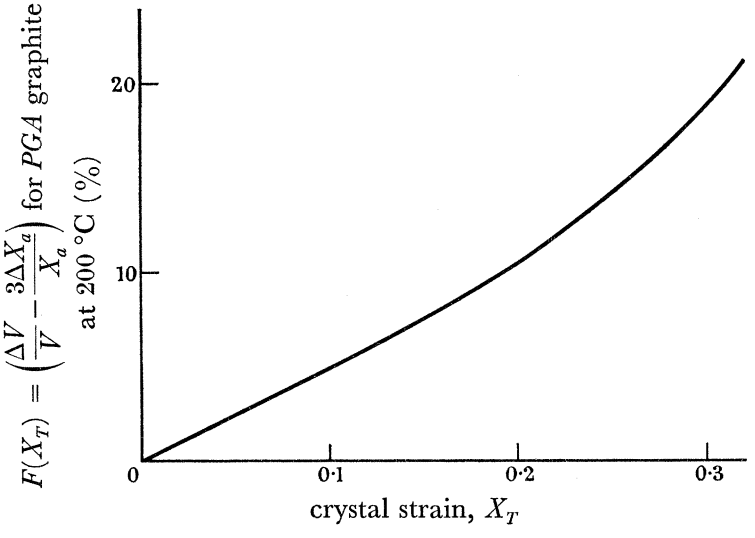

FIGURE 18. Variation of $F(X_T)$ with differential crystal strain X_T for *PGA* graphite irradiated at 200 °C.

than those in the pyrolytic material. On the other hand, above 250 °C the initial rates of *c* axis crystal strain with dose in pyrolytic material are larger than those in the *PGA* crystals, but the discrepancy decreases with dose. It appears therefore that only the concentration of small interstitial groups and single vacancies are different in the two materials, possibly as a result of interaction of the former with dislocations (cf. Woolley 1965).

When $\Delta X_c/X_c$ and $\Delta X_a/X_a$ are obtained as functions of dose at different temperatures from *PGA* graphite data, bulk dimensional change curves for other graphites at different temperatures can be constructed, with the aid of (1) and relations between A_x and X_T of the type shown in figure 16. At present, the high temperature data on other materials

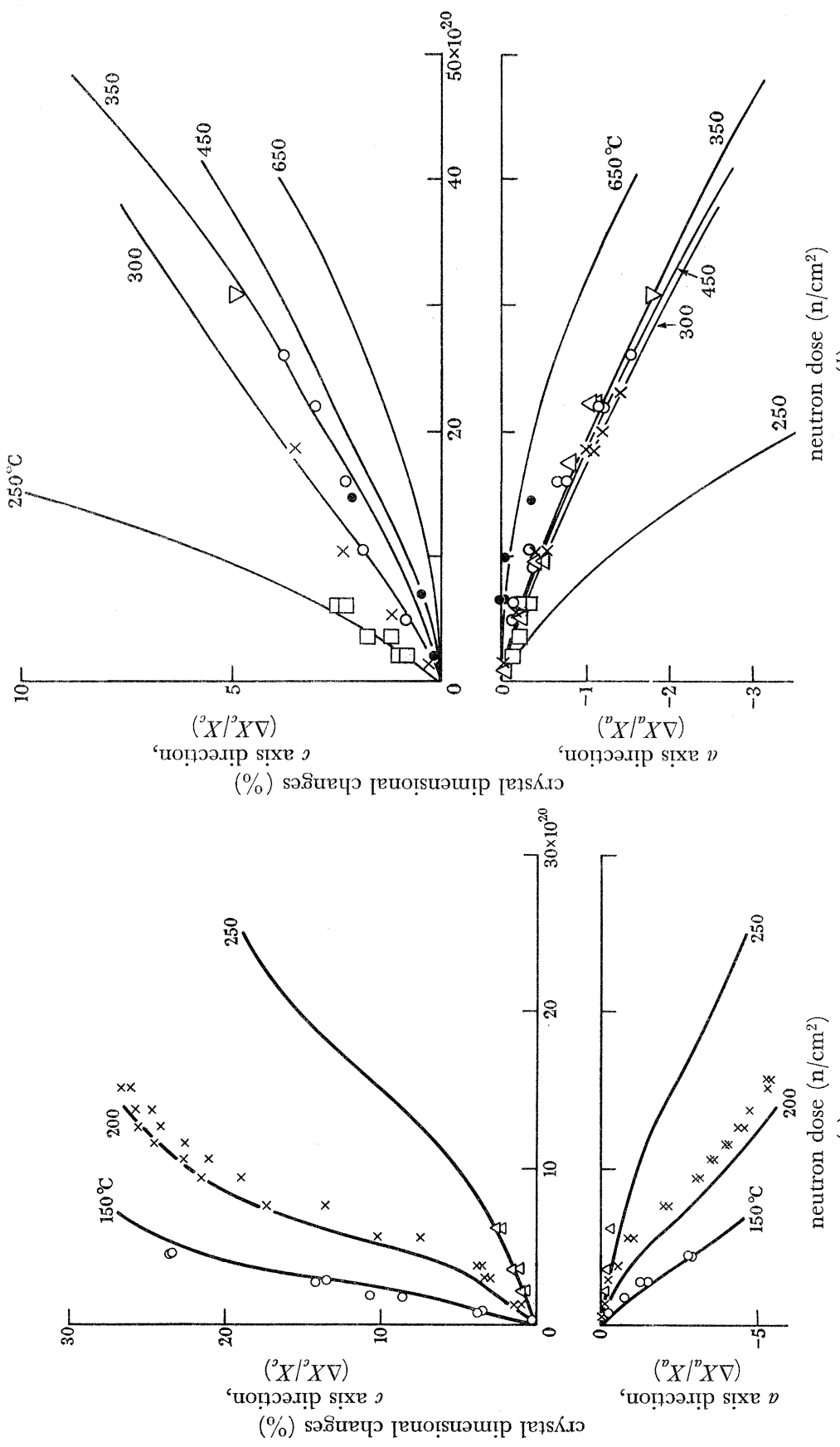

FIGURE 19. (*a*) Comparison of *PGA* crystal dimensional changes calculated from equations (3) and (4) with pyrolytic graphite dimensional changes for irradiation at 150 and 250 °C. Calculated *PGA* crystal dimensional changes at 200 °C, given in figure 13, are included. ○, 150 °C; ×, 200 °C; △, 250 °C.

(*b*) Comparison of *PGA* crystal dimensional changes calculated from equations (3) and (4) with pyrolytic graphite dimensional changes for irradiation in the temperature range 250 to 650 °C. □, 250 °C; △, 300 °C; ×, 350 °C; ▽, 400 to 450 °C (BR 2); ○, 450 °C; ●, 650 °C.

does not extend to large enough crystal strains for them to be a convincing test of the model; they still only extend to crystal strains at which (1) and (2) adequately represent their behaviour. This of course also applies to the *PGA* data at high temperatures.

The dimensional change behaviour of different graphites at high doses has been predicted recently (Williamson & Horner 1964). The present analysis shows that their predictions are based on incorrect values for the crystal dimensional changes and the A_x parameters. Their calculations have not been corrected by using the new values, because their analysis also specified the use of a dose scaling factor with temperature for $\Delta X_a/X_a$. Figure 19 shows that the shape of the curve of $\Delta X_a/X_a$ as a function of dose at 300 to 450 °C is not the same as that at 200 °C; hence the use of the scaling factor is unsound. Further, Williamson & Horner postulate that δ is independent of dose, which has now been shown (in the preceding paper) not to be true at 200 °C. Thus revised predictions of the growth behaviour of graphites at doses where the crystal dimensional changes are unknown must await the development of a better theory for predicting the crystal changes.

It is possible, however, to reach some broad conclusions which are extremely valuable. It has been shown (Kelly 1965) that, in the temperature range 300 to 800 °C, the parameter δ is high and that at 450 °C it has a value of 0·5. Under these conditions the crystals are changing in shape but not in volume and the process seems to be controlled by the formation of large interstitial clusters and the collapse of irregular lines of vacancies. It therefore seems likely that the rates of crystal strain with dose will not change significantly with neutron dose until large strains have been achieved and that the δ value will remain constant at 0·5. The dimensional changes in several graphites at 450 °C have been constructed in figure 20 by using the values of A_x given in figure 16 and by assuming that the crystal strain rates, obtained from figure 19, at 450 °C are independent of dose. For simplicity, it has been assumed that graphites *HM* and *RB* are perfectly isotropic and that the A_x values given in figure 16 apply in all directions. Figure 20 clearly shows that the high thermal expansion isotropic material *RB* suffers least shrinkage and that the maximum shrinkage should not exceed 1·8%, while the maximum shrinkage in the low thermal expansion isotropic graphite *HM* should not exceed 3%. Having reached their peak shrinkages, both of these graphites should start to expand owing to generation of porosity at high crystal strains. The anisotropic *PGA* material should have been a maximum shrinkage of about 2·0% in the perpendicular direction, but it is much more likely to exhibit growth at high doses than the *RB* material. Such growth has been observed at 800 °C (Helm 1964) in a material similar to *PGA*. In the parallel direction the *PGA* material can exhibit shrinkages of more than 6% and it is not possible at present to say what the maximum shrinkage will be.

At temperatures other than 450 °C where δ is less than 0·5, the maximum shrinkage values will be smaller and, at all temperatures, the doses required to achieve these maximum shrinkages will depend on the rates of crystal strain. At the same time, if complete isotropy is not obtained in the so-called isotropic graphites, represented by the moulded materials *RB* and *HM*, the curves for the preferred *c* axis direction would be above the mean curves given in figure 20, while curves in the other directions would lie below the mean curves.

This work highlights the importance of achieving both high thermal expansion coefficients and a high degree of isotropy in reactor graphites in order to minimize bulk dimensional changes at temperatures above 300 °C. Such graphites are being developed on a

commercial scale by the leading manufacturers of nuclear graphite in the United Kingdom for use in future graphite moderated reactors (Hutcheon & Thorne 1965).

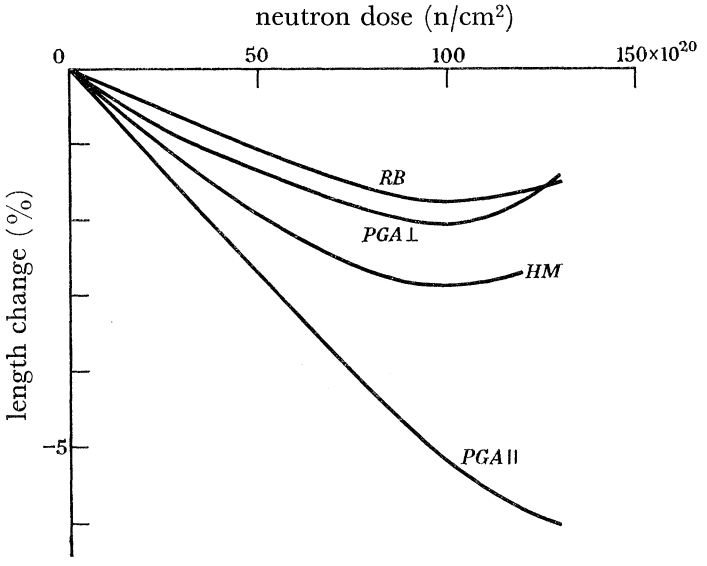

FIGURE 20. Predicted dimensional change behaviour of some graphites at 450 °C, assuming constant crystal dimensional change rates and using A_x values given in figure 16.

The data on which this work and that described in the preceding paper are based have been collected as the result of an extensive irradiation programme. It is a pleasure to acknowledge the enthusiastic support of the sections concerned, in particular of the Research Reactors Division at A.E.R.E. for performing the irradiations; of the Reactor Engineering Laboratory, Reactor Group, Risley for the design and construction of the irradiation furnaces; of the Irradiation Physics Section at Culcheth for undertaking most of the detailed measurements.

REFERENCES

Ashton, B. W. & Winton, J. 1961 U.K.A.E.A. TRG Report 128(C).

Brocklehurst, J. E & Bishop, R. A. 1964 *Carbon*, **2**, 27.

Bushong, R. M. & Neel, E. A. 1962 *Proc. Fifth Biennial Conference on Carbon*, **1**, 595. London: Pergamon Press.

Currie, L. M., Hamister, V. C. & MacPherson, H. G. 1955 *Proc. Int. Conf. on the Peaceful Uses of Atomic Energy*, A/CONF. 8/P/534.

Eatherley, W. P., Janes, M., Mansfield, R. L., Bourdeau, R. A. & Meyer, R. A. 1958 *Proc. Second U.N. Int. Conf. on the Peaceful Uses of Atomic Energy*, A/CONF. 15/P/708.

Goggin, P. R., Henson, R. W., Perks, A. J. & Reynolds, W. N. 1964 *Carbon*, **1**, 189.

Gray, B. S., Hanstock, R. F., Kelly, B. T. & Nettley, P. T. 1966 *Carbon*. To be published.

Helm, J. W. 1964 U.S.A.E.C. Report HW-71500B.

Hutcheon, J. M. & Jenkins, M. J. 1965 *Proc. S.C.I. Conference on Industrial Carbons and Graphites, London*. To be published.

Hutcheon, J. M. & Thorne, R. P. 1965 *Proc. S.C.I. Conference on Industrial Carbons and Graphites, London*. To be published.

Kelly, B. T. 1965 *Proc. S.C.I. Conference on Industrial Carbons and Graphites, London*. To be published.

Kelly, B. T., Jones, D. & James, A. 1962 *J. Nucl. Mater.* **7**, 279.

Kelly, B. T., Martin, W. H. & Nettley, P. T. 1966 *Phil. Trans.* A, **260**, 37 (preceding paper).

PHILOSOPHICAL TRANSACTIONS OF THE ROYAL SOCIETY A MATHEMATICAL, PHYSICAL & ENGINEERING SCIENCES

Legendre, P., Mondet, L., Arrongon, Ph., Cornuault, P., Gueron, J. & Hering, H. 1955 *Proc. Int. Conf. on the Peaceful Uses of Atomic Energy*, A/CONF. 8/P/343.
Martin, W. H., Kelly, B. T. & Nettley, P. T. 1962 *Nucl. Engng*, p. 484.
O'Driscoll, W. G. & Bell, J. C. 1960 *Materials for nuclear engineers*, p. 171. London: Temple Press.
Reynolds, W. N. 1965 *Phil. Mag.* **11**, 357.
Simmons, J. H. W. 1957 *Proc. Third Biennial Conference on Carbon*, p. 559. London: Pergamon Press.
Simmons, J. H. W. 1961 U.K.A.E.A., A.E.R.E. Report 3883.
Simmons, J. H. W., Kelly, B. T., Nettley, P. T. & Reynolds, W. N. 1964 *Proc. Third U.N. Int. Conf. on the Peaceful Uses of Atomic Energy*, A/CONF. 28/P/163.
Simmons, J. H. W. & Reynolds, W. N. 1962 Uranium and Graphite, *Monogr. Inst. Metals, London*, no. 27, p. 75.
Sutton, A. L. & Howard, V. C. 1962 *J. Nucl. Mater.* **7**, 58.
Thrower, P. A. 1964 *J. Nucl. Mater.* **12**, 56.
Williamson, G. K. & Horner, P. 1964 *J. Brit. Nucl. Energy Soc.* p. 269.
Woods, W. K., Bupp, L. P. & Fletcher, J. F. 1955 *Proc. Int. Conf. on the Peaceful Uses of Atomic Energy*, A/CONF. 8/P/746.
Woolley, R. L. 1965 *Phil. Mag.* **11**, 475.

PHILOSOPHICAL TRANSACTIONS OF THE ROYAL SOCIETY A MATHEMATICAL, PHYSICAL & ENGINEERING SCIENCES